Pyrrole-Based Narrow-Band-Gap Copolymers for Red Light-Emitting Diodes and Bulk Heterojunction Photovoltaic Cells

Mingliang Sun,[1,2] Li Wang,[1] Wei Yang[1]

[1]*Institute of Polymer Optoelectronic Materials and Devices, Key Laboratory of Special Functional Materials, South China University of Technology, Guangzhou 510640, People's Republic of China*
[2]*Institute of Material Science and Engineering, Ocean University of China, Qingdao 266100, People's Republic of China*

Received 20 January 2009; accepted 11 March 2010
DOI 10.1002/app.32416
Published online 3 June 2010 in Wiley InterScience (www.interscience.wiley.com).

ABSTRACT: A series of narrow-band-gap conjugated copolymers (PFO-DPT) derived from pyrrole, benzothiadiazole, and 9,9-dioctylfluorene (DOF) is prepared by the palladium-catalyzed Suzuki coupling reaction with the molar feed ratio of 4,7-bis(*N*-methylpyrrol-2-yl)-2,1,3-benzothiadiazole (DPT) around 1, 5, 15, 30, and 50%. The obtained polymers are readily soluble in common organic solvents. The solutions and the thin solid films of the copolymers absorb light from 300 nm to 600 nm with two absorbance peaks at around 380 nm and 505 nm. The PL emission consists mainly of DPT unit emission at around 624–686 nm depending on the DPT content in solid film. The EL emission peaks are red-shifted from 630 nm for PFO-DPT1 to 660 nm for PFO-DPT50. Bulk heterojunction photovoltaic cells fabricated from composite films of copolymer and [6,6]-phenyl C_{61} butyric acid methyl ester (PCBM) as electron donor and electron acceptor, respectively, in device configuration: ITO/PEDOT : PSS/PFO-DPT : PCBM/Ba/Al shows power conversion efficiencies 0.15% with open-circuit voltage (V_{oc}) of 0.60 V and short-circuit current density (J_{sc}) of 0.73 mA/cm^2 under AM1.5 solar simulator (100 mW/cm^2). J Appl Polym Sci 118: 1462–1468, 2010

Key words: 4,7-bis(*N*-methylpyrrol-2-yl)-2,1,3-benzothiadiazole; 9,9-dioctylfluorene; light-emitting diodes; solar cells

INTRODUCTION

In the last decades, conjugated polymers have absorbed considerable interest due to their excellent properties in electronic and optoelectronic aspects.[1] Many of these expectations have been realized by utilizing conjugated polymer materials making polymer light-emitting diodes,[2,3] polymer photovoltaic cells,[4–6] and field-effect transistors.[7,8] Polymer light-emitting diodes and polymer bulk heterojunction (BHJ) solar cell are among the most extensively investigated and prospective in future commercial applications. Among a wide range of conjugated polymers, polyfluorene (PF), polythiophene (PT), poly(para-phenylene-vinylenes) (PPV), and their derivatives have received considerable attentions for their exceptional optoelectronic properties. Up to now, there are very few reports about the application of pyrrole-based conjugated polymer for light-emitting diodes and photovoltaic cells. Recently, Janssen and Sariciftci report pyrrole and benzothiadiazole based conjugated polymer for photovoltaic cells application with ECE from 0.3% to 1%.[9–11]

In this article, we reported the synthesis and characterization of a series of new low-band-gap copolymers with pyrrole, benzothiadiazole, and 9,9-dioctylfluorene (DOF) with pyrrole under or up to 50% (molar percent) in the polymer. Red light-emitting devices and photovoltaic devices were fabricated from the obtained copolymers. The photovoltaic device is based on the composite thin films of the copolymer PFO-DPT and PCBM as an active layer.

EXPERIMENTAL

General methods and materials

^{1}H-NMR spectra were recorded on a Bruker DRX 300 spectrometer operating at 300 MHz and were referred to tetramethylsilane. GC-MS were obtained on GC-MS (TRANCE2000, Finnigan Co.). UV–vis absorption spectra were measured on a HP 8453 spectrophotometer. PL spectra in solutions and in thin solid films were taken by Fluorolog-3

Correspondence to: W. Yang (pswyang@scut.edu.cn).
Contract grant sponsor: National Natural Science Foundation of China; contract grant numbers: 50433030, 50903078 and 50990065.
Contract grant sponsor: Ministry of Science and Technology; contract grant number: 2009CB623600.

spectrofluorometer (Jobin Yvon) under 325 nm light excitation. The number average molecular weights of these polymers are determined by GPC using polystyrene as a standard and THF as eluent. Elemental analyses were performed on a Vario EL Elemental Analysis Instrument (Elementar Co.).

All reagents, unless otherwise specified, were obtained from Aldrich, Acros, and TCI Chemical Co. and used as received. All the solvents were further purified under a nitrogen flow. 4,7-bis(5′-bromo-*N*-methylpyrrol-2-yl)-2,1,3-benzothiadiazole (1), 2,7-dibromo-9,9-dioctylfluorene (2), and 2,7-bis(4,4,5,5-tetramethyl-1,3,2-dioxaborolan-2-yl)-9,9-dioctylfluorene (3) were prepared following the procedure described in Refs. 8 and 12, and characterized by the GC-MS and ^{1}H-NMR spectra.

Device fabrication and measurement

LED was fabricated on prepatterned indium-tin oxide (ITO) with a sheet resistance 10–20 Ω/□. The substrate was ultrasonically cleaned with acetone, detergent, deionized water, and 2-propanol subsequently. Oxygen plasma treatment was made for 10 min as the final step of substrate cleaning to improve the contact angle just before film coating. Onto the ITO glass a 50 nm-thick layer of polyethylenedioxythiophene-polystyrene sulfonic acid (PEDOT : PSS) film was spin-coated from its aqueous dispersion (Baytron P 4083, Bayer AG), aiming at improving the hole injection and avoiding the possibility of leakage. PEDOT : PSS film was dried at 80°C for 2 h in a vacuum oven. Then 40 nm-thick PVK layer was spin-coated on the top of the ITO/PEDOT : PSS surface from solution of the PVK in chlorobenzene. The emitting copolymers were spin-coated on the top of the ITO/PEDOT : PSS PVK surface inside dry box. The typical thickness of the emitting layer was 70–80 nm. A thin layer of barium as an electron injection cathode and the subsequent 180 nm-thick aluminum capping layers were thermally deposited by vacuum evaporation through a mask at a base pressure below 2×10^{-4} Pa. The deposition speed and thickness of the barium and aluminum layers were monitored by a thickness/rate meter (model STM-100, Sycon). The cathode area defined the active area of the device. The typical active area of the devices in this study was 0.15 cm^2. The spin coating of the EL layer and device performance tests were carried out within a glove box (Vacuum Atmosphere Co.) with nitrogen circulation. Current-luminance-voltage (*I-L-V*) characteristics were measured with a computerized Keithley 236 Source Measure Unit and calibrated Si photodiode. External quantum efficiency was verified by measurement in the integrating sphere (IS080, Lab sphere) and luminance was calibrated by PR705 spectragraph-photometer after the encapsulation of devices with UV-curing epoxy and thin cover glass. EL spectra were taken by InstaSpec^{TM} IV CCD spectragraph.

Energy conversion efficiencies of solar cells were measured under an AM1.5 solar simulator (100 mW/cm^2). The energy conversion efficiency (ECE) and fill factor (FF) were calculated by the following equations:

$$\mathrm{ECE} = \mathrm{FF} \times J_{sc} \times V_{oc}/P_{in} \quad (1)$$

$$\mathrm{FF} = J_m \times V_m/J_{sc} \times V_{oc} \quad (2)$$

Where P_{in} is the incident radiation flux, J_{sc} and V_{oc} are the short-circuit current density and open-circuit voltage, respectively, and J_m and V_m are the current density and voltage at the maximum power output, respectively.

Synthesis of polymer

Carefully purified 2,7-dibromo-9,9-dioctylfluorene (2), 2,7-bis(4,4,5,5-tetramethyl-1,3,2-dioxaborolan-2-yl)-9,9-dioctylfluorene (3), 4,7-bis(5′-bromo-*N*-methylpyrrol-2-yl)-2,1,3-benzothiadiazole (1), $(PPh_3)_4Pd(0)$ (0.5–2.0 mol %), and several drops of Aliquat 336 (methyl trioctyl ammonium chloride that worked as phase transfer catalyst) were dissolved in a mixture of toluene and aqueous 2*M* Na_2CO_3. The solution was refluxed with vigorous stirring for 36 h in an argon atmosphere. At the end of polymerization, the polymers were end-capped with 2,7-bis(4,4,5,5-tetramethyl-1,3,2-dioxaborolan-2-yl)-9,9-dioctylfluorene and bromobenzene. The mixture was then poured into methanol and the precipitated material was recovered by filtration and purified by flash column chromatography on silica gel (60 mesh) with toluene as eluent to remove the catalyst and the inorganic salts. The resulted polymers were air-dried overnight, followed by dried under vacuum. In the process of polymerization, the comonomer feed ratios of (2 + 3) to 1 were 99 : 1, 95 : 5, 85 : 15, 70 : 30, and 50 : 50, and the mole ratio of 2,7-bis-(4,4,5,5-tetramethyl-1,3,2-dioxaborolan-2-yl)-9,9-dioctylfluorene to 2,7-dibromo-9,9-dioctylfluorene and 4,7-bis(5′-bromo-*N*-methylpyrrol-2-yl)-2,1,3-benzothiadiazole was always remained as 3 : (1 + 2) = 1 : 1. The corresponding copolymers were named PFO-DPT1, 5, 15, 30, and 50, respectively.

PFO-DPT1

3 (0.50 equiv), 2 (0.49 equiv), and 1 (0.01 equiv) were used in this polymerization. ^{1}H-NMR (300 MHz, $CDCl_3$): 7.86–7.84, 7.69–7.61, 2.13, 1.26–1.15, 0.84–0.80. Elemental analyses: Found: C, 84.92; H, 9.76; S, 0.22; N, 1.45. The feed ratios of DOF/DPT is 99 : 1,

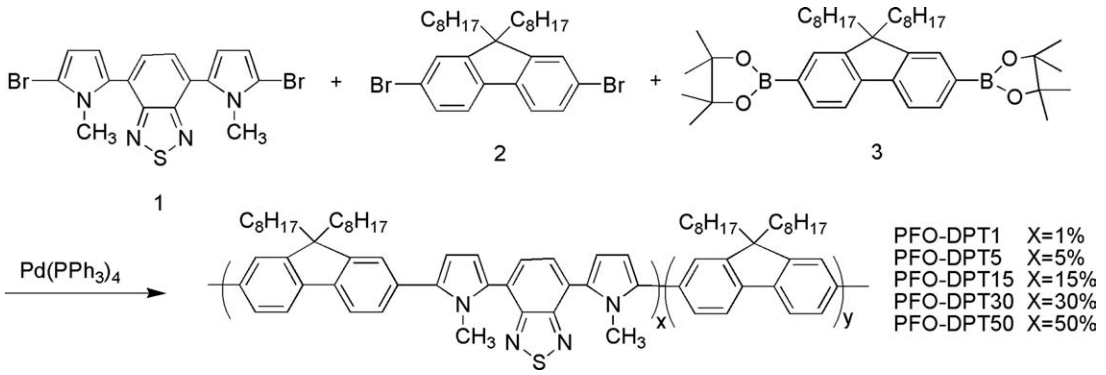

Figure 1 Synthesis route of the copolymers.

the actual DOF/DPT in the copolymers is 97.4 : 2.6 calculated from S element contents in the copolymers.

PFO-DPT5

3 (0.50 equiv), 2 (0.45 equiv), and 1 (0.05 equiv) were used in this polymerization. ^{1}H-NMR (300 MHz, $CDCl_3$): 7.87–7.85, 7.70–7.61, 3.76, 2.15, 1.27–1.16, 0.86–0.82. Elemental analyses: Found: C, 87.28; H, 9.86; S, 0.45; N, 1.73. The feed ratios of DOF/DPT is 95 : 5, the actual DOF/DPT in the copolymers is 94.6 : 5.4 calculated from S element contents in the copolymers.

PFO-DPT15

3 (0.50 equiv), 2 (0.35 equiv), and 1 (0.15 equiv) were used in this polymerization. ^{1}H-NMR (300 MHz, $CDCl_3$): 7.88–7.82, 7.77–7.70, 6.78, 6.58, 3.76, 2.13, 1.28–1.16. Elemental analyses: Found: C, 85.76; H, 9.48; S, 1.41; N, 2.89. The feed ratios of DOF/DPT is 85 : 15, the actual DOF/DPT in the copolymers is 83 : 17 calculated from S element contents in the copolymers.

PFO-DPT30

3 (0.50 equiv), 2 (0.20 equiv), and 1 (0.30 equiv) were used in this polymerization. ^{1}H-NMR (300 MHz, $CDCl_3$): 7.88– 7.82, 7.77–7.70, 6.78, 6.58, 3.76, 2.13, 1.28–1.16, 0.84–0.82. Elemental analyses: Found: C, 81.91; H, 8.79; S, 2.46; N, 4.56. The feed ratios of DOF/DPT is 70 : 30, the actual DOF/DPT in the copolymers is 70.2 : 29.8 calculated from S element contents in the copolymers.

PFO-DPT50

3 (0.50 equiv) and 1 (0.50 equiv) were used in this polymerization. ^{1}H-NMR (300 MHz, $CDCl_3$): 7.82–7.75, 7.57, 6.78, 6.58, 3.75, 2.10, 1.43, 1.28–1.12, 0.81. Elemental analyses: Found: C, 74.66; H, 7.61; S, 4.21; N, 6.67. The feed ratios of DOF/DPT is 50 : 50, the actual DOF/DPT in the copolymers is 49 : 51 calculated from S element contents in the copolymers.

RESULTS AND DISCUSSION

Synthesis and chemical characterization

The general synthetic routes toward the copolymers are outlined in Figure 1. The obtained copolymers are readily soluble in common organic solvents, such as toluene, THF, and chloroform. The number average molecular weights of these polymers are determined by GPC using a polystyrene standard, ranging from 5600 to 29,700 (16–78 repeat units in the polymer backbone) with a polydispersity index (M_w/M_n) between 1.86 and 3.34 (Table I). ^{1}H-NMR chemical shift of the polymer at 6.78, 6.58, and 3.75 ppm is attributed to DPT segment which intensity increasing with the increasing of DPT content in the backbone. This demonstrates that DPT unit is

TABLE I
UV–vis Absorption, Electrochemical Properties, Photoluminescence, and Molecular Weights of the Copolymers

Copolymers	$\lambda_{(Abs)max}$ (nm)	E_g (eV)	E_{ox} (V)	HOMO (eV)	LUMO (eV)	λ_{PL} (nm)	QE_{PL} (%)	M_n ($\times 10^3$)	M_w/M_n
PFO-DPT1	384	2.89	1.27	−5.67	−2.78	624	79	5.6	1.86
PFO-DPT5	385	2.02	1.27	−5.67	−3.65	650	74	29.7	2.61
PFO-DPT 15	387	2.00	1.24	−5.64	−3.64	658	30	14.2	2.67
PFO-DPT 30	386	1.99	1.18	−5.58	−3.59	660	19	8.0	2.45
PFO-DPT50	386	1.98	1.13	−5.53	−3.55	686	13	8.8	3.34

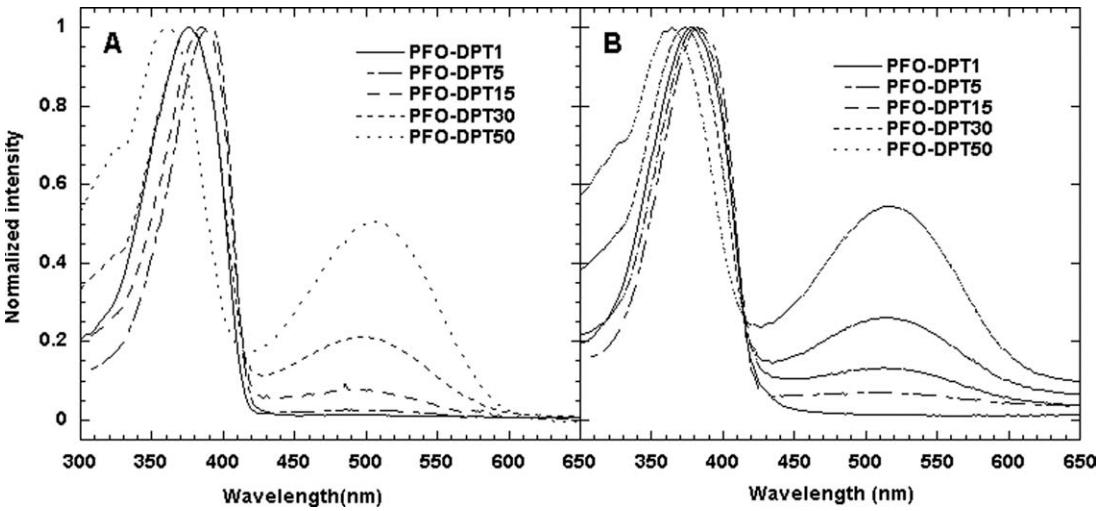

Figure 2 UV–vis absorption spectra in THF solution (A) and in solid film (B).

successfully incorporated into polyfluorene backbone. The actual ratios of substituted fluorene (DOF) to low-band-gap monomer (DPT) in the copolymers are estimated by elemental analysis (S content), which is in good agreement with the feed ratios of the monomers within experimental error.

Absorption properties and electrochemical characteristics

The UV–vis absorption properties of the conjugated polymers based on 9,9-dioctylfluorene (DOF) and 4,7-bis(*N*-methylpyrrol-2-yl)-2,1,3-benzothiadiazole (DPT) are presented in Table I. Figure 2 shows the normalized UV–vis absorption spectra of the polymers in the solutions of THF and in solid thin films. The absorption spectra of copolymers monitored both in solutions of THF and in solid thin films display two absorption bands. The absorption peaks around 380 nm are attributed to fluorene segments, and the absorption peaks around 505 nm are attributed to DPT units. The absorption intensity at 505 nm increases gradually with increasing content of DPT in the polymer backbone. The two distinguishable absorption features of the copolymers demonstrate again that DPT is successfully incorporated into polyfluorene backbone. For the UV–vis spectra of copolymer PFO-DPT1, the 505 nm peak from the DPT unit is not apparent in the solution and in thin solid film for its relatively low DPT contents.

The electrochemical properties of the copolymers were investigated by cyclic voltammetry (CV). Table I summarizes oxidation potentials derived from the onset in the cyclic voltammograms of the copolymers. We can record one p-doping process in the copolymers (PFO-DPT1, PFO-DPT5, and PFO-DPT15), and the onset of oxidation process of these copolymers is around 1.25 V, which is attributed to

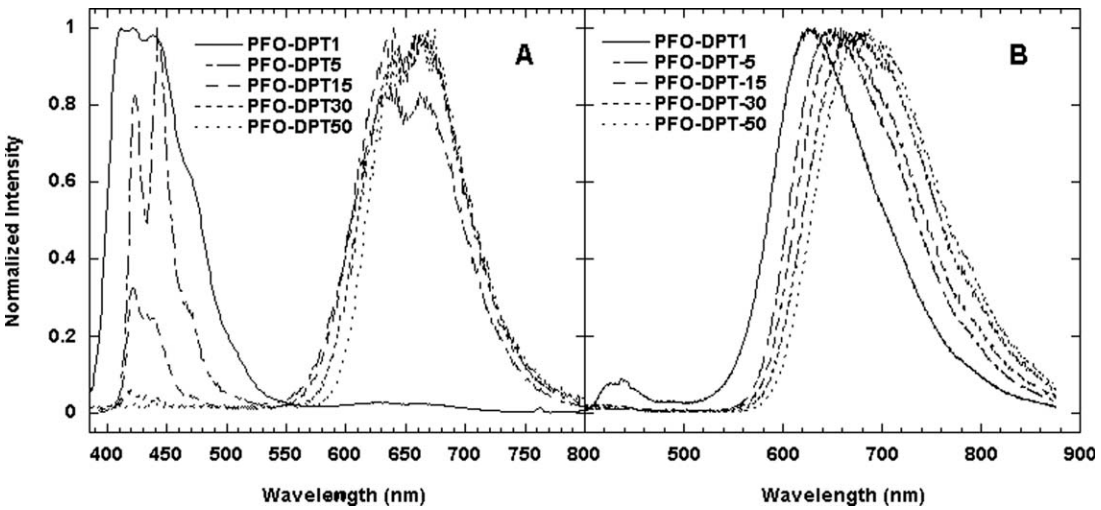

Figure 3 PL spectra in THF solution (A) and in solid film (B).

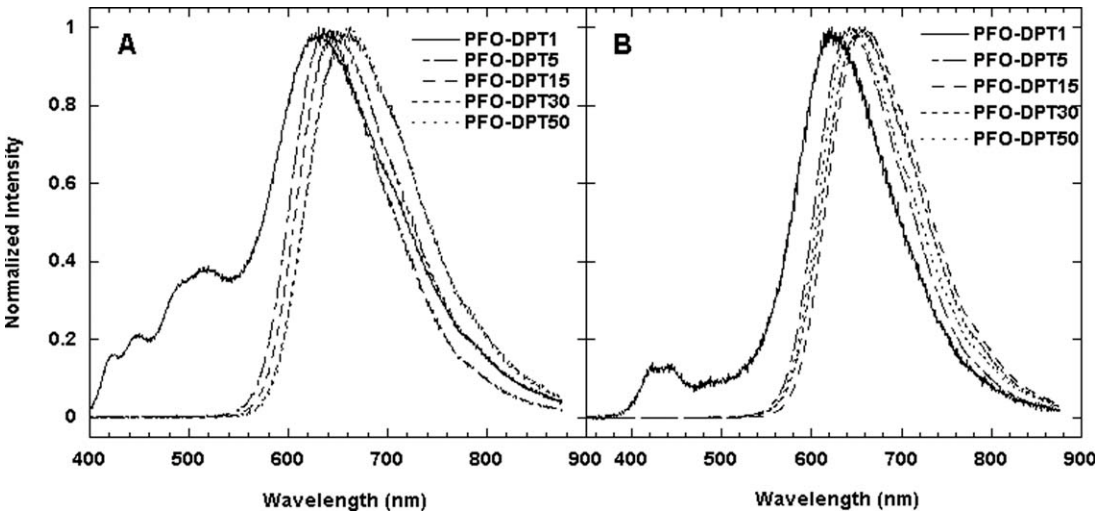

Figure 4 Normalized EL spectra with device configuration ITO/PEDOT : PSS/PFO-DPT/Ba/Al (A) or ITO/PEDOT : PSS/PVK/PFO-DPT/Ba/Al (B).

the oxidation process of the DOF segment in the copolymers. For the copolymer PFO-DPT30 and PFO-DPT50, oxidation onset were observed at around 1.15 V corresponding to the oxidation process of the DPT segment. The optical band-gap (E_g in Table I) is estimated from the onset wavelength of UV–vis spectra of the copolymer in solid film. HOMO and LUMO levels calculated by empirical formulas $E_{\mathrm{HOMO}} = -e\ (E_{\mathrm{ox}} + 4.4)$ (eV) and $E_{\mathrm{LUMO}} = -e\ (E_{\mathrm{HOMO}} + E_g)$ (eV) are also listed in Table I.[13]

Photoluminescence properties

Figure 3(A) shows the normalized PL spectra of the polymers in the solutions of THF at 1×10^{-3} mol/L. The PL spectrum of PFO-DPT1 has three peaks at about 421, 438, and 633 nm, which are attributed to DOF and DPT segment, respectively. The PL spectrum of PFO-DPT5 and PFO-DPT15 are similar with PFO-DPT1 with increased DPT emission. We cannot monitor emission from DOF in the PL spectra of PFO-DPT30 and PFO-DPT50 in the solutions, and PL emission peak is 669 and 674 nm, respectively.

Figure 3(B) shows the normalized PL spectra of the polymers in solid thin films. PL emission of PFO-DPT1 in solid film is similar to that in THF solutions with decreasing PFO PL intensity. PL spectra of PFO-DPT5, 15, 30, and 50 in solid film show exclusively DPT emission at around 650–686 nm depending on the DPT content. The shapes of the PL spectra for copolymers with different DPT content (5–50%) are very similar, and the PL peaks are

TABLE II
Device Performances at Maximum External Quantum Efficiency of the Copolymers (ITO/Hole Transport Layer/Polymer/Ba/Al)

Copolymers	Hole transport layer	V_{th}[a] (V)	$\mathrm{QE}_{\mathrm{max}}$[b] (%)	L[c] (cd/m^2)	LE[d] (cd/A)	CIE (x,y)[e]
PFO-DPT1	PEDOT : PSS	4.95	0.01	31	0.01	0.65,0.34
	PEDOT : PSS/PVK	8.5	0.16	224	0.12	0.65,0.34
PFO-DPT5	PEDOT : PSS	8.8	0.25	189	0.15	0.65,0.36
	PEDOT : PSS/PVK	12.2	0.43	338	0.26	0.65,0.34
PFODPT15	PEDOT : PSS	6.3	0.10	139	0.06	0.65,0.34
	PEDOT : PSS/PVK	7.7	0.29	382	0.17	0.66,0.34
PFO-DPT30	PEDOT : PSS	6.3	0.08	125	0.05	0.67,0.33
	PEDOT : PSS/PVK	8.5	0.27	329	0.17	0.66,0.34
PFO-DPT50	PEDOT : PSS	7.0	0.12	210	0.07	0.67,0.33
	PEDOT : PSS/PVK	7.8	0.14	163	0.08	0.65,0.34

[a] Threshold voltage.
[b] Maximum external quantum efficiency.
[c] Luminance.
[d] Luminance efficiency.
[e] CIE.

TABLE III
Device Characteristics of PFO-DPT + PCBM PVC Devices

Active layer	J_{sc} (mA/cm^2)	V_{oc} (V)	FF (%)	ECE (%)
PFO-DPT30/PCBM (1 : 4)	0.26	0.55	28.8	0.04
PFO-DPT50/PCBM (1 : 4)	0.73	0.60	34.5	0.15

significantly red-shifted with increasing DPT content in the copolymers, from 624 nm for the copolymer with 1% DPT content to 686 nm for the alternating copolymer. The PL quantum efficiencies of the polymer film obtained under 325 nm excitation of the HeCd laser are also listed in Table I.

Electroluminescent properties

Electroluminescent devices based on PFO-DPT copolymers are fabricated with configuration as ITO/PEDOT : PSS/PFO-DPT/Ba/Al. Figure 4(A) shows EL spectra of the copolymers in such devices. Fluorene host emission and excimer emission are not quenched completely in the copolymer PFO-DPT1, when incorporate only as low as 1% DPT units into copolymers chain. This indicates that energy trapping process (from fluorene segment to DPT unit) is not as fast and efficient as in the other copolymers.[3] The EL emission peaks are red-shifted from 630 nm for PFO-DPT1 to 660 nm for PFO-DPT50.

Because the HOMO for the copolymer is around (−5.5)–(−5.7) eV (Table I), whereas the work function of PEDOT is around (−5.0)–(−5.2) eV, it would be possible to expect a better hole injection once PVK [work function (−5.5)–(−5.6) eV] is used as the hole injection interlayer. We further fabricated EL devices with a configuration ITO/PEDOT : PSS/PVK/PFO-DPT/Ba/Al, which show similar EL spectra with the above mentioned devices and enhanced device performance. Figure 4(B) shows EL spectra of the copolymers in such devices. Table II show polymer based light-emitting device performance.

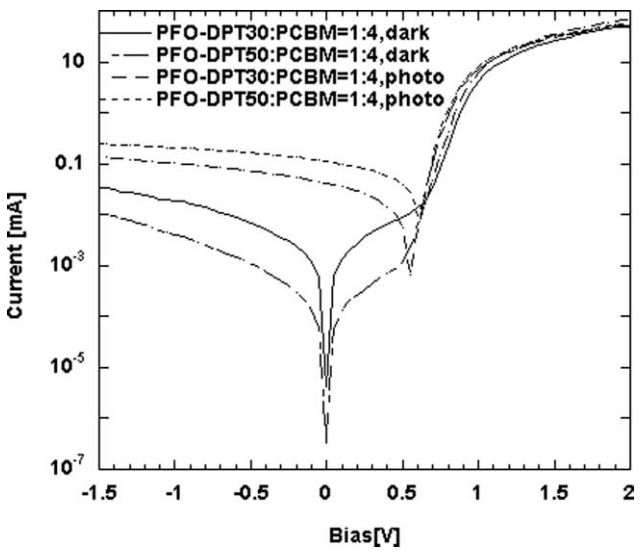

Figure 5 The *I–V* characteristic of the PVC based on the device ITO/PEDOT : PSS/PFO-DPT + PCBM/Ba/Al.

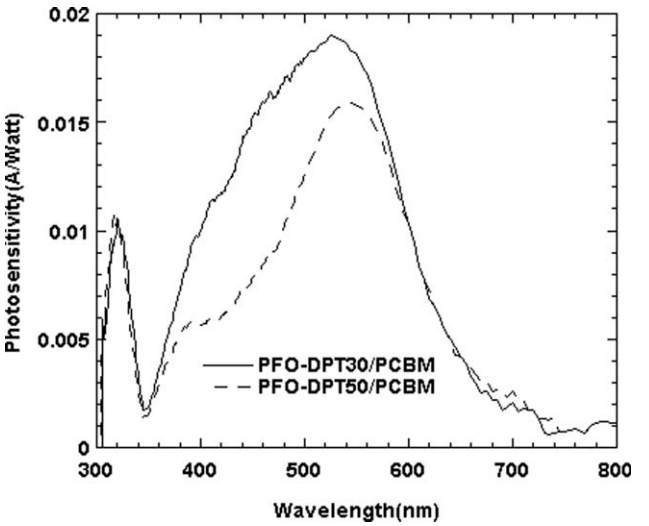

Figure 6 Photosensitivity of PVCs based on PFO-DPT/PCBM blend.

Characteristics of photovoltaic devices

Bulk heterojunction polymer photovoltaic cells (PPVCs) are made up of copolymers (PFO-DPT30 and PFO-DPT50) as the donor phase blending with PCBM as the acceptor phase with a sandwich configuration of ITO/PEDOT : PSS/PFO-DPT : PCBM/Ba/Al. Table III lists the PFO-DPT + PCBM based PPVCs device performance. The best PPVCs device performance obtained from the device based on PFO-DPT50 : PCBM (1 : 4) blend is J_{sc} 0.73 mA/cm^2, V_{oc} 0.60 V, and η_e (ECE) 0.15% under AM1.5 illuminator (100 mW/cm^2). The *I–V* characteristics of device based on ITO/PEDOT : PSS/PFO-DPT + PCBM/Ba/Al is shown in Figure 5. The photocurrent response wavelengths of the PVCs based on PFO-DPT + PCBM blends covers 300–700 nm (Fig. 6).

CONCLUSIONS

We synthesized a series of new conjugated copolymers PFO-DPT, composed of pyrrole, benzothiadiazole, and 9,9-dioctylfluorene (DOF) via a palladium-catalyzed Suzuki coupling reaction. The PLED device with these polymers as the emitting layer shows saturated red emission. The best bulk heterojunction polymer photovoltaic cells (PPVCs) shows

power conversion efficiencies 0.15% with open-circuit voltage (V_{oc}) of 0.60 V and short-circuit current density (J_{sc}) of 0.73 mA/cm^2 under AM 1.5 solar simulator (100 mW/cm^2).

References

1. Forrest, S. R.; Thompson, M. E. Chem Rev 2007, 107, 923.
2. Lo, S. C.; Burn, P. L. Chem Rev 2007, 107, 1097.
3. Hou, Q.; Xu, Y. S.; Yang, W.; Yuan, M.; Peng, J. B.; Cao, Y. J Mater Chem 2002, 12, 2887.
4. Günes, S.; Neugebauer, H.; Sariciftci, N. S. Chem Rev 2007, 107, 1324.
5. Li, G.; Shrotriya, V.; Huang, J.; Yao, Y.; Moriarty, T.; Emery, K.; Yang, Y. Nat Mater 2005, 4, 864.
6. Sun, M. L.; Wang, L.; Xia, Y. J.; Du, B.; Liu, R. S.; Cao, Y. Acta Polym Sin 2007, 10, 952.
7. Murphy, A. R.; Fréchet, J. M. J. Chem Rev 2007, 107, 1066.
8. Sun, M. L.; Lan, L. F.; Wang, L.; Peng, J. B.; Cao, Y. Macromol Chem Phys 2008, 209, 2504.
9. Brabec, C. J.; Winder, C.; Sariciftci, N. S.; Hummelen, J. C.; Dhanabalan, A.; van Hal, P. A.; Janssen, R. A. J. Adv Funct Mater 2002, 12, 709.
10. Dhanabalan, A.; van Hal, P. A.; van Duren, J. K. J.; van Dongen, J. L. J.; Janssen, R. A. J. Synth Met 2001, 119, 169.
11. van Duren, J. K. J.; Dhanabalan, A.; van Hal, P. A.; Janssen, R. A. F. J. Synth Met 2001, 121, 1587.
12. Ranger, M.; Rondeau, D.; Leclerc, M. Macromolecules 1997, 30, 7686.
13. Li, Y. F.; Cao, Y.; Gao., J.; Wang, D. L.; Yu, G.; Heeger, A. J. Synth Met 1999, 99, 243.